

MODES IN CURVED STEP-INDEX OPTICAL FIBRES

Indexing terms: Optical fibres, Optical-waveguide theory

By using parabolic, instead of circular, cylindrical co-ordinates the field distributions of the natural modes of curved step-index fibres can be described completely, yet simply. The mode caustics corresponding to the geometrical guiding limit of the equivalent rays of a curved fibre can be clearly demonstrated. Near-field mode patterns and caustics obtained experimentally are in excellent agreement with the theory.

Introduction: Analyses of propagation in curved optical fibres normally assume^{1,2} that the modes approximate to those of a straight fibre. However, it has been shown theoretically^{3,4} that the field distributions are considerably deformed by bending, and experimental confirmation of this result is presented here (Fig. 2). Theoretical studies of the 'real' modes of a curved fibre have proved rather complex, involving, for example, a double Fourier-Bessel-series expansion³ or a perturbation method,⁴ in terms of circular cylindrical co-ordinates. However, the results are not easy to assimilate without complex numerical calculations.

In experimental studies of propagation in curved fibres⁵ it was noted that the near-field and far-field radiation patterns are not circularly symmetric, or even circular, but that the modal field distribution is parabolic in shape. In the same way

that one uses circular cylindrical, and not rectangular, co-ordinates to study modes in a uniformly circular system such as a straight fibre, it seemed worth while, in view of the observed mode patterns, to attempt to analyse a curved fibre in terms of a parabolic system. As a result, we find that by invoking parabolic cylindrical co-ordinates the modes and the caustics of a curved fibre can be simply and accurately obtained. The method gives a clear insight into the mode structure and is in excellent agreement with experimentally observed field patterns.

Theory: From the weak-guidance approximation and the conformal-mapping technique for the field of the guided modes, Marcuse has shown³ that the transverse field component E can be obtained from the scalar wave equation

$$\nabla^2 E + (kn)^2 (1 + 2r \cos \theta/R) E = 0 \quad (1)$$

where n is the refractive index, R is the radius of curvature and k is the free-space wave number. If, now, parabolic cylindrical co-ordinates (μ, λ, z) are used,* instead of the usual circular cylindrical co-ordinates (r, θ, z) , together with the relations

$$\mu = (2r)^{1/2} \sin(\theta/2) \quad \text{and} \quad \lambda = (2r)^{1/2} \cos(\theta/2) \quad (2)$$

then using the technique of separation of variables the scalar wave equation can be written

$$E = \eta(\lambda) \xi(\mu) \exp(-j\beta z) \quad (3)$$

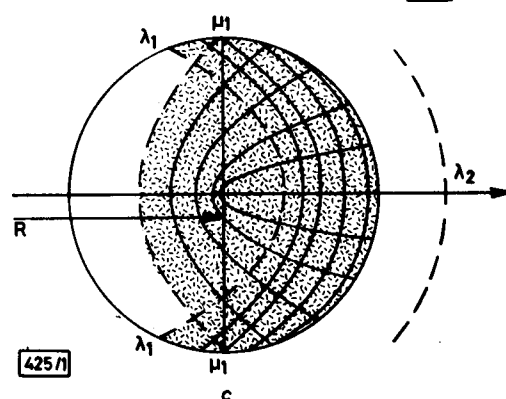
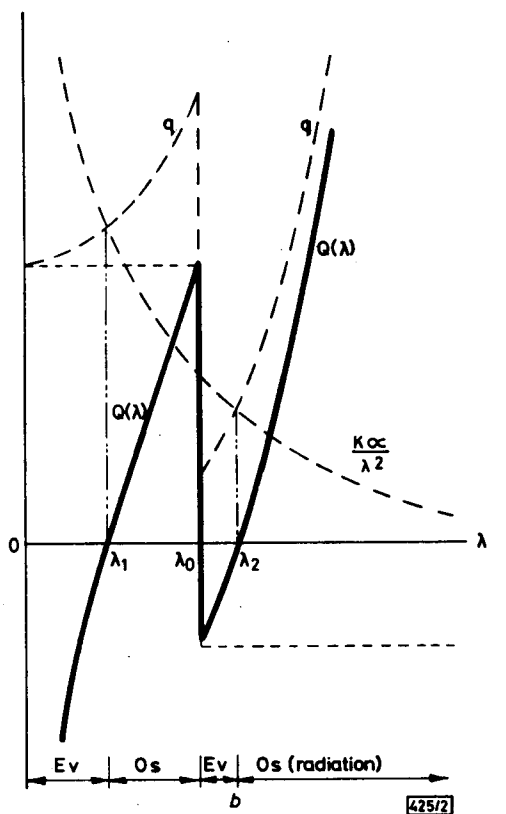
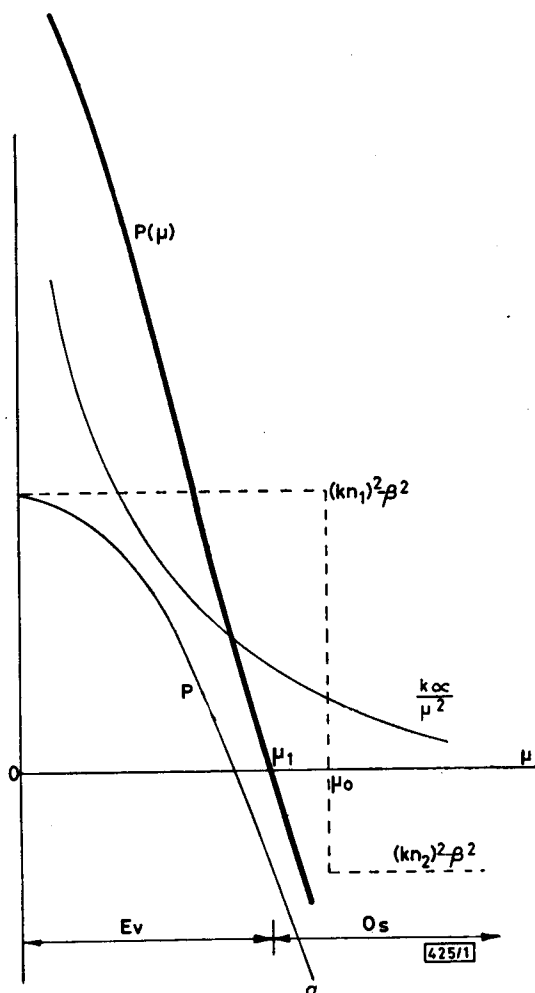


Fig. 1
 a Variation of $P(\mu)$ and its components with μ . Os and Ev denote regions of oscillation and evanescent fields, respectively. The core-cladding interface is denoted by μ_0 and $p = (kn_1)^2 - \beta^2 - (kn\mu)^2/R$
 b Variation of $Q(\lambda)$ and its components with λ . The core-cladding interface is denoted by λ_0 and $q = (kn)^2 - \beta^2 + (kn\lambda)^2/R$
 c Schematic of mode lines in curved fibre of bend radius R

* Throughout this letter, λ is used as the standard symbol for a parabolic co-ordinate and not to denote wavelength

72

where $\eta(\lambda)$ and $\xi(\mu)$ are the solutions of the differential equations

$$\left. \begin{aligned} \frac{d^2 \xi(\mu)}{d\mu^2} + \mu^2 P(\mu) \xi(\mu) &= 0, \\ \frac{d^2 \eta(\lambda)}{d\lambda^2} + \lambda^2 Q(\lambda) \eta(\lambda) &= 0 \end{aligned} \right\} \quad (4)$$

having the separation constant α , and

$$\left. \begin{aligned} P(\mu) &= (kn)^2 - \beta^2 - (kn)^2 \mu^2 / R + k\alpha / \mu^2 \\ Q(\lambda) &= (kn)^2 - \beta^2 + (kn)^2 \lambda^2 / R - k\alpha / \lambda^2 \end{aligned} \right\} \quad (5)$$

These equations can be used to find the eigenfunctions (η , ξ) and the eigenvalues (α , β). Since the eigenfunctions are independent, the field distribution of a guided mode can be completely described by the parabolic co-ordinates. We show here only the schematic of the mode pattern, which is compared with those obtained experimentally; more detailed calculations will be presented elsewhere.

With the help of the WKB method it is found that there are regions of oscillating fields, corresponding to $Q(\lambda) > 0$, $P(\mu) > 0$, and evanescent fields, $Q(\lambda) < 0$, $P(\mu) < 0$, as indicated by the plots of $P(\mu)$ against μ and $Q(\lambda)$ against λ in Figs. 1a and b. It can be seen that in the μ direction there is a caustic at $\mu = \pm\mu_1$ and the locations of the evanescent field and the oscillating field are shown schematically in Fig. 1c, relative to the core of the fibre and the centre of curvature. Similarly, in the λ direction a periodic field exists for $\lambda_1 < \lambda < \lambda_0$, where λ_0 is the value of λ at the core-cladding boundary. There is a second caustic at $\lambda = \lambda_2$, beyond which the radiation corresponding to bend loss appears. As expected, the radiation is emitted, and a shift of energy in the core occurs, in the direction away from the centre of curvature, as illustrated in Fig. 1c.

Experiment: Experimental confirmation of the theory presented above has been obtained during studies of the bending loss in single-mode fibres. The fibres were given a silicone-rubber coating having a refractive index lower than that of the cladding, which thus acted as the core of a multimode step-index fibre. The inner core of this 3-layer structure acted as the excitation source, since the bend-loss studies have shown⁵ that when the cladding of a single-mode fibre has a finite thickness the HE_{11} mode couples with the LP_{1m} cladding modes. As the volume of the single-mode core is small compared with that of the cladding, these cladding modes can be thought of as the core modes of the step-index, silicone-clad, multimode fibre.

Another factor to be borne in mind is that the cladding modes excited in a single-mode fibre depend strongly on the spot size of the HE_{11} mode, which, in turn, is directly related to the numerical aperture (n.a.) of the single-mode fibre, and on the cladding/core diameter ratio C . Two typical near-field patterns in a curved multimode fibre are shown in Figs. 2a and b for n.a._s = 0.094, $C = 26$ and n.a._s = 0.063, $C = 18$, respectively. In each case the numerical aperture of the multimode fibre is 0.333 and the bend radius R is 15 mm. It can be shown⁵ that higher cladding modes are excited with higher values of n.a._s, and this is evident from the photographs. The mode in Fig. 2a contains five lobes in the μ direction and seven in the λ direction and the parabolic shape of the former can be clearly seen. In this case the energy (rays) propagates without striking the core-cladding interface on the inside of the bend and the caustic separating the oscillation and evanescent regions is well inside the core. In contrast, because of the smaller diameter (83 μm compared with 133 μm in Fig. 2a), the rays still strike the interface on the inside of the bend for the fibre in Fig. 2b. There are five lobes in the μ direction, starting near the inside bend wall. The parabolic shape is evident in the three λ lobes. Thus both Figs. 2a and b comprise a combination of two parabolic mode patterns, although the λ lobes in Fig. 2a look circular because of the higher value of λ there. It is interesting to note that the far-

field pattern in Fig. 2c, which was obtained for the same fibre and conditions as in Fig. 2a, is similar to those illustrated by Kapany.⁶

Conclusions: The field distribution in a curved fibre can be simply and clearly analysed by using parabolic cylindrical co-ordinates. The theory presented is in good qualitative agreement with experiment. Parabolic co-ordinates have apparently been used previously⁷ to calculate bend loss, but no details are given. It should be possible to make a direct measurement of

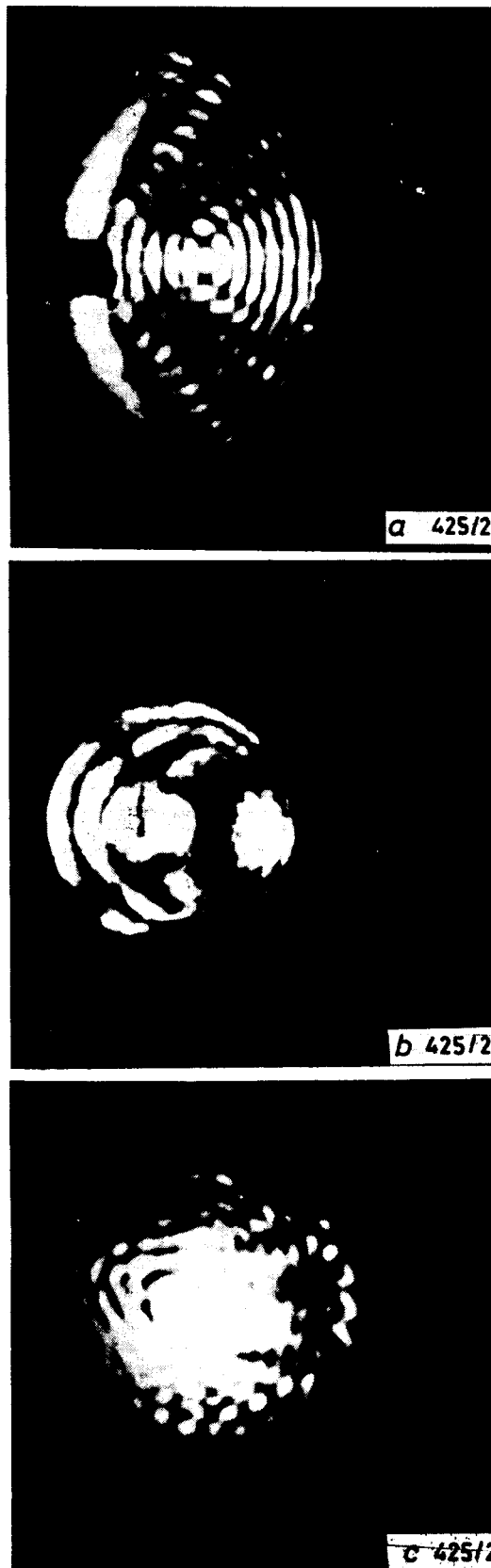


Fig. 2 Near-field (a) and far-field (c) mode patterns of multimode fibre of core diameter 136 μm , n.a. = 0.333 and bend radius = 15 mm

The near-field pattern in (b) is for a fibre of core diameter 86 μm and n.a._s = 0.063

the axial propagation constant by observing the positions of the two caustics μ_1 and λ_1 and solving eqn. 5. Detailed theoretical and experimental results will be reported elsewhere.

Acknowledgments: We are indebted to S. R. Norman for fabricating the fibres, and to D. N. Payne for helpful discussions. Grateful acknowledgment is also made to the Pirelli General Cable Company for the award of a research fellowship and to the UK Science Research Council for supporting the work.

W. A. GAMBLING
H. MATSUMURA

5th August 1977

Department of Electronics
University of Southampton
Southampton SO9 5NH, England

References

- 1 LEWIN, L.: 'Radiation from curved dielectric slabs and fibres' *IEEE Trans.*, 1974, MTT-22, pp. 718-727
- 2 SNYDER, A. W., WHITE, I., and MITCHELL, D. J.: 'Radiation from bent optical waveguides', *Electron. Lett.*, 1975, 11, pp. 332-333
- 3 MARCUSE, D.: 'Field deformation and loss caused by curvature of optical fibres', *J. Opt. Soc. Am.*, 1976, 66, pp. 311-320
- 4 MIYAGI, M., and YIP, G. L.: 'Field deformations and polarisation change in a step-index optical fibre due to bending', *Opt. & Quantum Electron.*, 1976, 8, pp. 335-341
- 5 MATSUMURA, H.: unpublished work
- 6 KAPANY, N. S.: 'Fiber optics' (Academic Press, New York, 1967), p. 333
- 7 GLOGE, D.: 'Propagation effects in optical fibres', *IEEE Trans.*, 1975, MTT-23, pp. 106-120